

DESY 97-037
December 1997

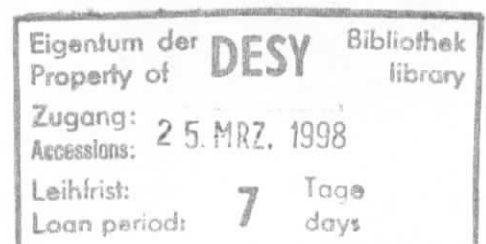
Testing the Strong W -System at the LHC & Linear Colliders

H.-J. He

Deutsches Elektronen-Synchrotron DESY, Hamburg



ISSN 0418-9833





TESTING THE STRONG W -SYSTEM AT THE LHC & LINEAR COLLIDERS

HONG-JIAN HE

Theory Division, Deutsches Elektronen-Synchrotron DESY
D-22603 Hamburg, Germany
E-mail: hjhe@desy.de

ABSTRACT

In the absence of a light Higgs boson, the new physics effects of the strong electroweak symmetry breaking (EWSB) must show up at the TeV scale and can be generally described by a complete set of the chiral Lagrangian parameters. After analyzing the current bounds on these EWSB parameters, we present a global classification on probing all of them at the LHC and the high energy linear colliders (LC). Then, we focus on the precision test of the quartic gauge boson interactions at the TeV LC. Special attention is put on how to probe the new $SU(2)_C$ -violation effects which are still poorly bounded by the current data. Finally, the interplay of the bi-gauge-boson and triple-gauge-boson productions in probing the EWSB dynamics is revealed and analyzed.

1. Strong EWSB Dynamics and its Model-Independent Description

Though the elementary Higgs boson (as the cornerstone of the standard model) has been sought in vain at LEP/SLD and Tevatron so far, its mass may be too heavy or merely a cutoff at the TeV scale beyond which the new physics must show up. The absence of a light Higgs results in a strongly coupled electroweak symmetry breaking (EWSB) sector, for which the usual perturbation theory breaks down and the electroweak chiral Lagrangian (EWCL) provides the most economic and general description of the new physics effects. This is one of the most important applications of the general idea about effective field theories^{1,2}. The EWCL is based upon the low energy derivative expansion with an effective cutoff Λ ($\leq 4\pi f_\pi \simeq 3.1\text{TeV}$) covering the main energy-reaches of the LHC (at the parton-level) and the planned TeV linear colliders (LC). By noting the fact that a simply scaled-up techni- ρ from QCD has a mass around 2TeV, it is suggested that the new physics threshold (the possible new heavy resonance) for the strong EWSB is very likely to lie around the end of the main energy ranges of the LHC/LC or just above it. This arises a *greater* challenge to the future colliders to decisively probe the EWSB mechanism at the TeV scale, and makes the non-resonance EWCL approach important and *complementary* to the direct resonance-studies (which are often model-dependent)^{3,4,5}.

Up to the next-to-leading order, the EWCL can be generally formulated as^{6,7}

$$\begin{aligned} \mathcal{L}_{\text{eff}} &= \mathcal{L}_0 + \mathcal{L}'_{\text{eff}} = [\mathcal{L}_G + \mathcal{L}_F + \mathcal{L}^{(2)}] + [\mathcal{L}^{(2)'} + \sum_{n=1}^{14} \mathcal{L}_n] \\ \mathcal{L}'_{\text{eff}} &\equiv \sum_n \alpha_n \hat{\mathcal{O}}_n \equiv \sum_n \ell_n \frac{f_\pi^{r_n}}{\Lambda^{a_n}} \mathcal{O}_n(W_{\mu\nu}, B_{\mu\nu}, D_\mu U, U, f, \bar{f}), \end{aligned} \quad (1)$$

where $\mathcal{L}_G = -\frac{1}{4}W_{\mu\nu}^a W^{a\mu\nu} - \frac{1}{4}B_{\mu\nu}B^{\mu\nu}$ and \mathcal{L}_F denotes the fermionic part. In (1), $U = \exp[i\tau^a \pi^a / f_\pi]$ and π^a is the would-be Goldstone boson (GB) field. $f_\pi \simeq 246$ GeV and the effective cut-off $\Lambda (\leq 4\pi f_\pi \simeq 3.1\text{TeV})$. The explicit expressions for nonlinear bosonic operators in \mathcal{L}_{eff} have been given by Refs. ^{6,7}, in which the leading-order operator $\mathcal{L}^{(2)} = \frac{1}{4}f_\pi^2 \text{Tr}[(D^\mu U)(D_\mu U)^\dagger]$ is universal, and the next-to-leading order (NLO) operators $\mathcal{L}^{(2)'}$, $\mathcal{L}_{1\sim 11}$ (CP -conserving) and $\mathcal{L}_{12\sim 14}$ (CP -violating) are model-dependent. Here, the dimensionless coefficients ℓ_n 's for these NLO operators are related to the corresponding notations α_n 's in Ref. ⁶ by definition $\alpha_n \equiv \left(\frac{f_\pi}{\Lambda}\right)^2 \ell_n$. From the theoretical expectation, the ℓ_n 's are naturally around $O(1)$.²

2. Current Bounds on the EWSB Parameters

According to our recent global analysis, the updated current bounds on the EWSB parameters (ℓ_n 's) can be summarized as follows⁷. Here, $\Lambda_0 \equiv 4\pi f_\pi \simeq 3.1\text{TeV}$.

(i). Oblique corrections (LEP 2σ bounds)

$$\begin{cases} S = -0.36 \pm 0.19, \\ T = -0.03 \pm 0.26, \\ U = -0.31 \pm 0.54; \end{cases} \Rightarrow \begin{cases} -0.34 \left(\frac{\Lambda}{\Lambda_0}\right)^2 \leq \ell_0 \leq 0.30 \left(\frac{\Lambda}{\Lambda_0}\right)^2, \\ -0.063 \left(\frac{\Lambda}{\Lambda_0}\right)^2 \leq \ell_1 \leq 2.33 \left(\frac{\Lambda}{\Lambda_0}\right)^2, \\ -2.42 \left(\frac{\Lambda}{\Lambda_0}\right)^2 \leq \ell_8 \leq 4.37 \left(\frac{\Lambda}{\Lambda_0}\right)^2. \end{cases} \quad (2)$$

(ii). Triple gauge couplings (TGC)

• 1σ bounds from LEP global fit:

$$\begin{cases} -0.064 \leq \Delta g_1^Z \leq -0.002, \\ -0.046 \leq \Delta \kappa_Z \leq 0.042, \\ 0.0 \leq \Delta \kappa_\gamma \leq 0.112; \end{cases} \Rightarrow \begin{cases} -12.1 \left(\frac{\Lambda}{\Lambda_0}\right)^2 \leq \ell_2 \leq 32.3 \left(\frac{\Lambda}{\Lambda_0}\right)^2, \\ -18.5 \left(\frac{\Lambda}{\Lambda_0}\right)^2 \leq \ell_3 \leq 0.61 \left(\frac{\Lambda}{\Lambda_0}\right)^2, \\ -13.3 \left(\frac{\Lambda}{\Lambda_0}\right)^2 \leq \ell_9 \leq 18.5 \left(\frac{\Lambda}{\Lambda_0}\right)^2. \end{cases} \quad (3)$$

• Tevatron 2σ bounds:

$$\begin{cases} -1.1 \leq \Delta \kappa_V \leq 1.3, \\ -1.2 \leq \Delta g_1^Z \leq 1.2; \end{cases} \Rightarrow \begin{cases} -346 \left(\frac{\Lambda}{\Lambda_0}\right)^2 \leq \ell_3 \leq 346 \left(\frac{\Lambda}{\Lambda_0}\right)^2, \\ -412 \left(\frac{\Lambda}{\Lambda_0}\right)^2 \leq \ell_9 \leq 488 \left(\frac{\Lambda}{\Lambda_0}\right)^2. \end{cases} \quad (4)$$

(iii). Quartic gauge couplings (QGC)

At the current colliders, the QGCs cannot be tested at the tree-level (cf. Table 1 in Sec. 3). So far, only some simple estimates have been made by inserting them into the 1-loop corrections and keeping the log-terms only.^a Here is an updated estimate at 90% C.L. by choosing $\Lambda = 2$ TeV.

$$\begin{aligned} -4.0 \leq \ell_4 \leq 19.8, & \quad -9.9 \leq \ell_5 \leq 50.2, \\ -0.66 \leq \ell_6 \leq 3.5, & \quad -5.1 \leq \ell_7 \leq 25.8, \quad -0.67 \leq \ell_{10} \leq 3.4. \end{aligned} \quad (5)$$

^aThe ignored constant contributions plus the new loop counter-terms are of the same order of magnitude as the log-terms. So, some uncertainties (like a factor of 2 or so) may naturally exist in these estimates. Hence, it is crucial to further test them directly at the LHC and LC.

3. Global Analysis on Probing the EWSB Parameters at the LHC and LC

The coefficients (ℓ_n 's) of the 15 NLO operators depend on the details of the underlying dynamics and reflect the new physics. As shown in Sec. 2, except for $\ell_{0,1,8}$ (S, T, U), the current data only bound a few TGCs to $O(10)$ at the 1σ -level and give no direct tree-level bound on QGCs. The simple estimates of the bounds from 1-loop corrections still allow QGCs to be of $O(10)$. For a *complete* test of the EWSB sector in discriminating different dynamical models, all these TGCs and QGCs (ℓ_n 's) have to be measured through various high energy VV -fusion and $f\bar{f}^{(\prime)}$ -annihilation processes. ($V^a = W^\pm, Z^0$.) What is usually done in the literature is to consider only a small subset of these operators at a time for simplicity. The important question to ask is: "How and to what extent can one measure *all* the NLO coefficients ℓ_n at future colliders to *fully* explore the EWSB sector?" To answer this question, as the first step, one should (i). find out, for each given NLO operator, whether it can be measured via leading and/or sub-leading amplitudes of relevant processes at each collider; (ii). determine whether a given NLO operator can be sensitively (or marginally sensitively) probed through its contributions to the leading (or sub-leading) amplitudes of the relevant scattering process at each given collider; (iii). determine whether carrying out the above study for various high energy colliders can *complementarily* cover all the 15 NLO operators to probe the strongly interacting EWSB sector. For this purpose, a systematic global analysis has been performed in Refs.^{7,8} which reveals the important overall physical pictures and guide us for further elaborate precise numerical studies (cf. Sec. 4-5). In performing such a global analysis we developed a precise electroweak power counting rule (à la Weinberg) for estimating all high energy scattering amplitudes and formulated the equivalence theorem (ET)⁹ as a necessary physical criterion for sensitively probing the EWSB dynamics. Some important results are summarized into Fig. 1 and Table 1. Fig. 1 shows that, at the 14TeV LHC with $\int \mathcal{L} = 100\text{fb}^{-1}$ Luminosity and for $\Lambda = 2\text{TeV}$, the W^+W^+ -fusion is most sensitive to $\ell_{4,5}$ (QGCs) and marginally sensitive to $\ell_{3,9,11,12}$; while the $q\bar{q}' \rightarrow W^+Z$ annihilation can best probe $\ell_{3,11,12}$ and marginally test $\ell_{8,9,14}$. As further globally classified in Table 1, the VV -fusions and $f\bar{f}^{(\prime)}$ -annihilations are *complementary* in probing the different sets of these NLO parameters for both the LHC and LCs.

From this global analysis, we speculate that before having a large number of signal events at the LHC (i.e. with large integrated luminosity), the LHC alone will not be able to sensitively measure all these operators, the LC is needed to *complementarily* cover the rest of the NLO operators. In fact, the different phases of 500 GeV and 1.5 TeV energies at the LC are necessary because they will be sensitive to different NLO operators in the EWCL. An electron-photon (or a photon-photon) collider is also very useful for measuring all the NLO operators which discriminate different models of the EWSB in the strongly interacting scenario.

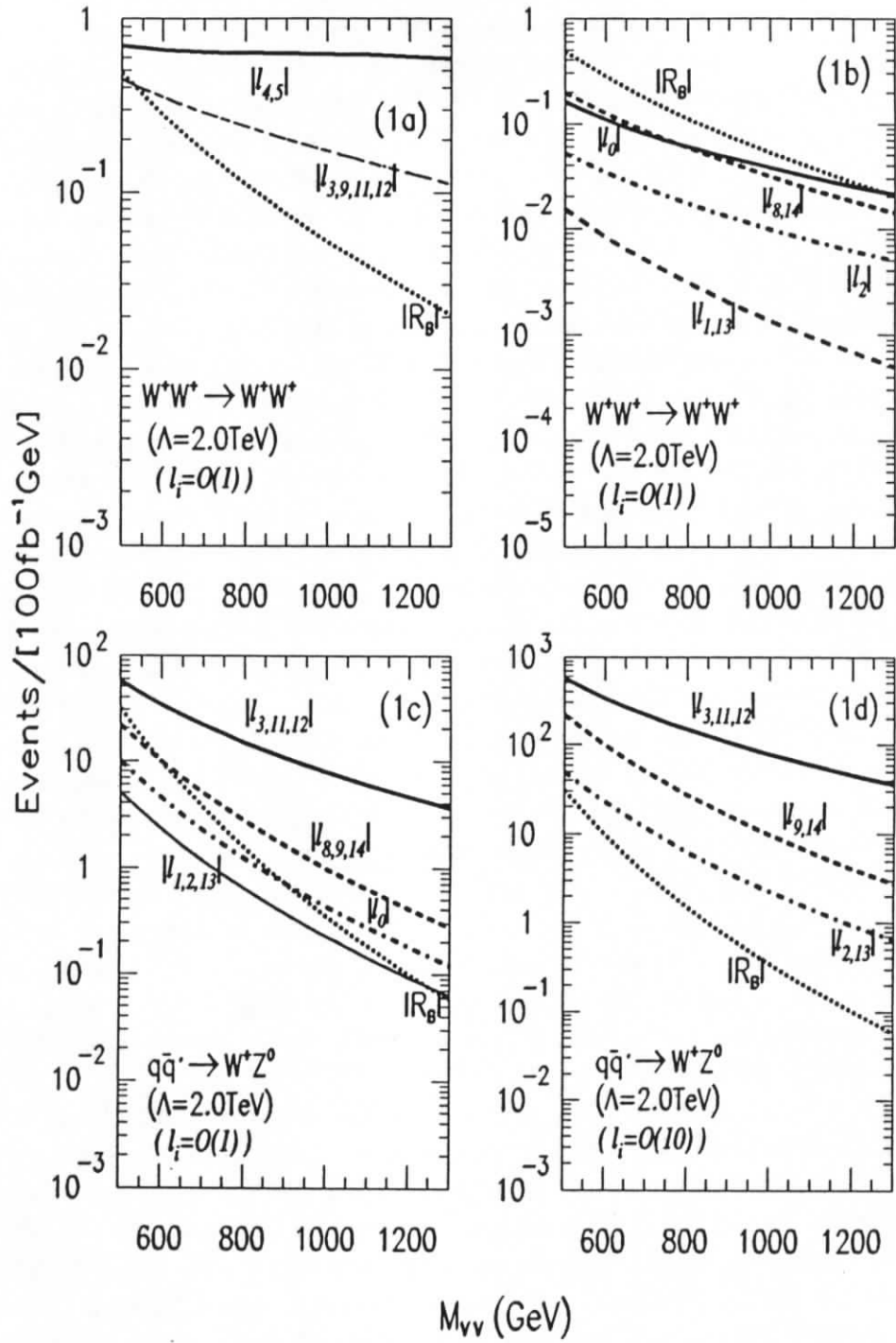


Fig.1. A classification of the 15 NLO operators at the LHC for $\Lambda=2.0\text{TeV}$.

Table 1. Probing the EWSB Sector at High Energy Colliders: A Global Classification for the NLO Bosonic Operators

(Notations: \checkmark = Leading contributions, Δ = Sub-leading contributions, and \perp = Low-energy contributions. Notes: † Here, \mathcal{L}_{13} or \mathcal{L}_{14} does not contribute at $O(1/\Lambda^2)$. ‡ At LHC(14), $W^+W^+ \rightarrow W^+W^+$ should also be included.)

Operators	$\mathcal{L}^{(2)}$	$\mathcal{L}_{1,13}$	\mathcal{L}_2	\mathcal{L}_3	$\mathcal{L}_{4,5}$	$\mathcal{L}_{6,7}$	$\mathcal{L}_{8,14}$	\mathcal{L}_9	\mathcal{L}_{10}	$\mathcal{L}_{11,12}$	$T_1 \parallel B$	Processes	
LEP-I (S,T,U)	\perp	\perp	\perp				\perp				$g^4 \frac{f^2}{\Lambda^2}$	$e^-e^+ \rightarrow Z \rightarrow f\bar{f}$	
LEP-II	\perp	\perp	\perp				\perp				$g^4 \frac{f^2}{\Lambda^2}$	$e^-e^+ \rightarrow W^-W^+$	
LC(0.5)/LHC(14)		Δ	\checkmark	Δ			Δ	\checkmark		Δ	$g^2 \frac{E^2}{\Lambda^2} \parallel g^2 \frac{M_W^2}{E^2}$ $g^3 \frac{E^2 f^2}{\Lambda^2} \parallel g^2 \frac{M_W^2}{E^2}$	$f\bar{f} \rightarrow W^-W^+/(LL)$ $f\bar{f} \rightarrow W^-W^+/(LT)$	
LC(1.5)/LHC(14)		Δ	\checkmark	Δ	\checkmark	Δ	Δ	\checkmark		\checkmark	$g^2 \frac{1}{f^*} \frac{E^2}{\Lambda^2} \parallel g^3 \frac{M_W^2}{E^2}$ $g^3 \frac{E^2}{\Lambda^2} \parallel g^3 \frac{M_W^2}{E^3}$ $g^2 \frac{1}{f^*} \frac{E^2}{\Lambda^2} \parallel g^3 \frac{M_W^2}{E^2}$ $g^3 \frac{E^2}{\Lambda^2} \parallel g^3 \frac{f^2}{\Lambda^2} \frac{M_W^2}{E^2}$ $\frac{E^2 E^2}{f^* \Lambda^2} \parallel g^2$ $\frac{E^2 E^2}{f^* \Lambda^2} \parallel g^2 \frac{M_W^2}{E^2}$ $\frac{E^2 E^2}{f^* \Lambda^2} \parallel g^2$ $\frac{E^2 E^2}{f^* \Lambda^2} \parallel g^2 \frac{M_W^2}{E^2}$ $\frac{E^2 E^2}{f^* \Lambda^2} \parallel g^2 \frac{M_W^2}{E^2}$ $\frac{E^2 E^2}{f^* \Lambda^2} \parallel g^2 \frac{M_W^2}{E^2}$ $\frac{E^2 E^2}{f^* \Lambda^2} \parallel g^2 \frac{M_W^2}{E^2}$	$f\bar{f} \rightarrow W^-W^+Z/(LLL)$ $f\bar{f} \rightarrow W^-W^+Z/(LLT)$ $f\bar{f} \rightarrow ZZZ/(LLL)$ $f\bar{f} \rightarrow ZZZ/(LLT)$ $W^-W^\pm \rightarrow W^-W^\pm/(LLLL)^\dagger$ $W^-W^\pm \rightarrow W^-W^\pm/(LLLT)^\dagger$ $W^-W^+ \rightarrow ZZ \& \text{perm.}/(LLLL)$ $W^-W^+ \rightarrow ZZ \& \text{perm.}/(LLLT)$ $ZZ \rightarrow ZZ/(LLLL)$ $ZZ \rightarrow ZZ/(LLLT)$	
		Δ	\checkmark	Δ	\checkmark	Δ	Δ	\checkmark		\checkmark	$g^2 \frac{E^2}{\Lambda^2} \parallel g^2 \frac{M_W^2}{E^2}$ $g^3 \frac{E^2 f^2}{\Lambda^2} \parallel g^2 \frac{M_W^2}{E^2}$ $g^2 \frac{1}{f^*} \frac{E^2}{\Lambda^2} \parallel g^3 \frac{M_W^2}{E^2}$ $g^3 \frac{E^2}{\Lambda^2} \parallel g^3 \frac{M_W^2}{E^3}$ $g^2 \frac{1}{f^*} \frac{E^2}{\Lambda^2} \parallel g^3 \frac{M_W^2}{E^2}$ $g^3 \frac{E^2}{\Lambda^2} \parallel g^3 \frac{f^2}{\Lambda^2} \frac{M_W^2}{E^2}$ $\frac{E^2 E^2}{f^* \Lambda^2} \parallel g^2$ $\frac{E^2 E^2}{f^* \Lambda^2} \parallel g^2 \frac{M_W^2}{E^2}$ $\frac{E^2 E^2}{f^* \Lambda^2} \parallel g^2$ $\frac{E^2 E^2}{f^* \Lambda^2} \parallel g^2 \frac{M_W^2}{E^2}$ $\frac{E^2 E^2}{f^* \Lambda^2} \parallel g^2 \frac{M_W^2}{E^2}$ $\frac{E^2 E^2}{f^* \Lambda^2} \parallel g^2 \frac{M_W^2}{E^2}$	$q\bar{q}' \rightarrow W^\pm Z/(LL)$ $q\bar{q}' \rightarrow W^\pm Z/(LT)$ $q\bar{q}' \rightarrow W^-W^+W^\pm/(LLL)$ $q\bar{q}' \rightarrow W^-W^+W^\pm/(LLT)$ $q\bar{q}' \rightarrow W^\pm ZZ/(LLL)$ $q\bar{q}' \rightarrow W^\pm ZZ/(LLT)$	
		Δ	\checkmark	Δ	\checkmark	Δ	Δ	\checkmark		\checkmark	$eg^2 \frac{E^2}{\Lambda^2} \parallel eg^2 \frac{M_W^2}{E^2}$ $eg^2 \frac{E^2}{\Lambda^2} \parallel eg^2 \frac{M_W^2}{E^2}$	$e^- \gamma \rightarrow \nu_e W^- Z/(LL)$ $e^- \gamma \rightarrow e^- W^- W^+/(LL)$	
		Δ	\checkmark	Δ	\checkmark	Δ	Δ	\checkmark		\checkmark			
		Δ	\checkmark	Δ	\checkmark	Δ	Δ	\checkmark		\checkmark			
		Δ	\checkmark	Δ	\checkmark	Δ	Δ	\checkmark		\checkmark			
		Δ	\checkmark	Δ	\checkmark	Δ	Δ	\checkmark		\checkmark			
		Δ	\checkmark	Δ	\checkmark	Δ	Δ	\checkmark		\checkmark			
		Δ	\checkmark	Δ	\checkmark	Δ	Δ	\checkmark		\checkmark			
		Δ	\checkmark	Δ	\checkmark	Δ	Δ	\checkmark		\checkmark			
LHC(14)		Δ	\checkmark	Δ	\checkmark	Δ	Δ	\checkmark		\checkmark			
LC($e^- \gamma$)		\checkmark	\checkmark	\checkmark	\checkmark	\checkmark	\checkmark	\checkmark		\checkmark			

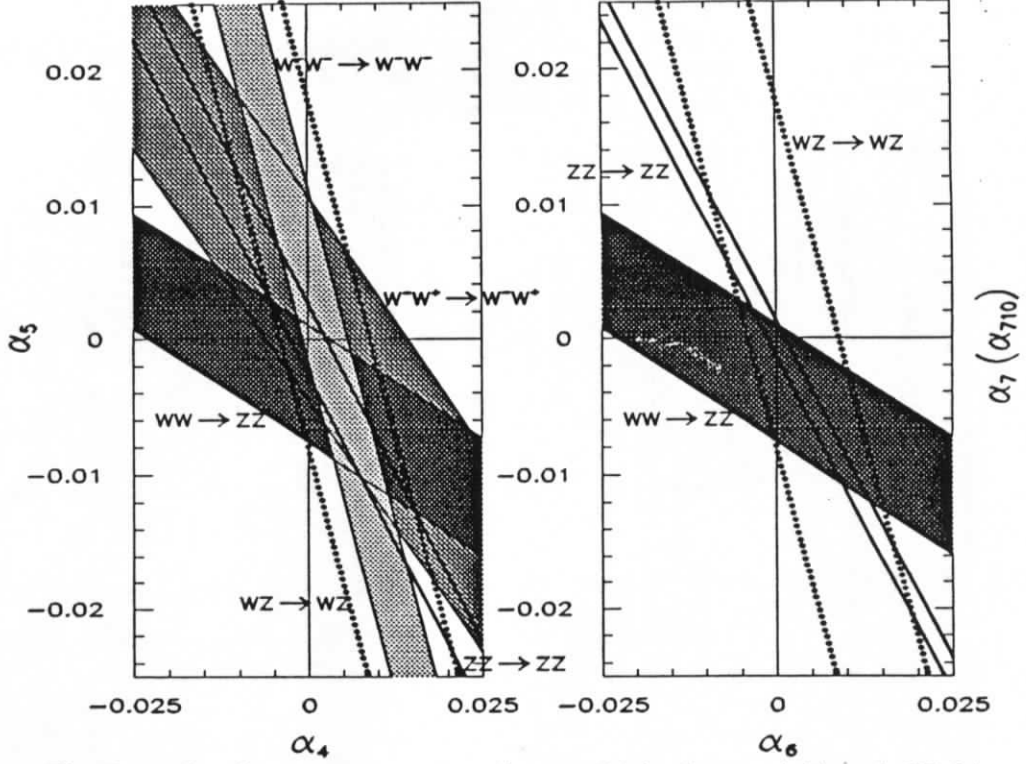


Fig.2. Unitarity bounds on α_n from V V fusions at $E_{VV}=1.5\text{TeV}$.

4. Precision Test of Quartic Gauge Couplings: VV-Fusions at the LC

There are five NLO operators $\mathcal{L}_{4,5}$ and $\mathcal{L}_{6,7,10}$ in (1) which contain the QGCs only and cannot be directly tested via TGCs at low energies.

$$\begin{cases} \mathcal{L}_4 = \alpha_4 [\text{Tr}(\mathcal{V}_\mu \mathcal{V}_\nu)]^2, \\ \mathcal{L}_5 = \alpha_5 [\text{Tr}(\mathcal{V}_\mu \mathcal{V}^\mu)]^2; \end{cases} \quad (SU(2)_C : \checkmark)$$

$$\begin{cases} \mathcal{L}_6 = \alpha_6 [\text{Tr}(\mathcal{V}_\mu \mathcal{V}_\nu)] \text{Tr}(\mathcal{T} \mathcal{V}^\mu) \text{Tr}(\mathcal{T} \mathcal{V}^\nu), \\ \mathcal{L}_7 = \alpha_7 [\text{Tr}(\mathcal{V}_\mu \mathcal{V}^\mu)] \text{Tr}(\mathcal{T} \mathcal{V}_\nu) \text{Tr}(\mathcal{T} \mathcal{V}^\nu), \\ \mathcal{L}_{10} = \alpha_{10} \frac{1}{2} [\text{Tr}(\mathcal{T} \mathcal{V}^\mu) \text{Tr}(\mathcal{T} \mathcal{V}^\nu)]^2. \end{cases} \quad (SU(2)_C : \times) \quad (6)$$

Here, $\mathcal{T} = U \tau_3 U^\dagger$ is the $SU(2)_C$ -violation operator. According to the ET⁹, these QGCs are most sensitive to the underlying Goldstone boson dynamics which governs the EWSB. In the absence of a light Higgs boson, the $V_L V_L \rightarrow V_L V_L$ fusions violate the unitarity at the TeV scale, signaling the necessity of new physics that is responsible for the strong EWSB. Within the EWCL up to including the NLO operators, the unitarity sensitively bounds these EWSB parameters through the $V_L V_L \rightarrow V_L V_L$ fusions at the TeV scale. The s -wave bounds are most restrictive and are globally shown in Fig. 2(a)-(b) for $SU(2)_C$ conserving and violating parameters, respectively. It is

interesting to note how the different VV -channels unitarily bound different regions of the parameter space.

While the LHC will give the first direct test on these QGCs, the large backgrounds limit its sensitivity to the parameter- α_n 's and cutting off these backgrounds significantly reduces the event rate. It was shown in Ref. ^{3,4} that even for the resonance-scenario only about 10 signal events were predicted for $W^\pm W^\pm$ channels at the LHC with a 100fb^{-1} luminosity after imposing necessary cuts in the gold-plated modes (i.e., pure leptonic decays). The corresponding study at a TeV e^-e^+ LC opens a much more exciting possibility^{4,10,11}. Here, we focus on how to make further precision tests for the more difficult non-resonance scenario at the LC. We have performed a systematic study by two computational approaches which are complementary to each other. One is the automatic CompHEP package¹⁵ for calculating the full tree-level $ee \rightarrow ff'VV$ processes. This is useful for computing the full standard model (SM) backgrounds in finding the complete set of kinematic cuts. The number of the background-diagrams in each channel is typically of $O(40 - 50)$ which makes the CompHEP-calculation a time-consuming and tedious task^{14, b}. The outcome is fully similar to the findings in Ref.^{10,4} since the kinematic cuts are mainly for cutting off the SM backgrounds and are insensitive to the fine structures of the strong VV -fusion signals. This was demonstrated in Ref.^{3,10} for the resonance-scenario at both the LHC and LC. The same strategy as Ref.¹⁰ is followed in our present analysis¹⁴ for suppressing the backgrounds. Another much more convenient approach is to use the effective- W method (EWA)^{12,13}. Note that the cross section of the whole fusion process $f_1 + f_2 \rightarrow f'_1 + f'_2 + X$ at the c.m. energy \sqrt{s} can be factorized into the product of two parts: (i). the probability function $f_{f/V_{\lambda_j}}(x)$ for finding a vector boson V_{λ_j} [with helicity λ_j ($j = 1, 2$)] inside the incoming fermion f_j ; (ii). the hard vector boson scattering cross section $\hat{\sigma}(V_{\lambda_1}^a + V_{\lambda_2}^b \rightarrow X|\hat{s})$ at the reduced c.m. energy $\hat{s} \equiv x \cdot s$. So, we have

$$d\sigma(f_1 + f_2 \rightarrow f'_1 + f'_2 + X|s) = \int_{x_{\min}}^1 dx \sum_{\lambda_j} \mathcal{P}_{f_1 f_2 / V_{\lambda_1}^a V_{\lambda_2}^b}(x) d\hat{\sigma}(V_{\lambda_1}^a + V_{\lambda_2}^b \rightarrow X|\hat{s}) \quad (7)$$

$$\mathcal{P}_{f_1 f_2 / V_{\lambda_1}^a V_{\lambda_2}^b}(x) = \int_x^1 \frac{dz}{z} f_{f_1 / V_{\lambda_1}^a}(z) f_{f_2 / V_{\lambda_2}^b}(x/z)$$

where $\mathcal{P}_{f_1 f_2 / V_{\lambda_1}^a V_{\lambda_2}^b}(x)$ is the luminosity of the VV -pair from incoming fermions and we have formulated it as the convolution of the distributions of these two gauge bosons. By (7), the computation of fusion-type signals are greatly simplified since there are only about 1–5 such diagrams for each channel. To get reliable numerical predictions, we emphasize that it is important to (i) further improve the V_T -luminosities which are quite inaccurate in the usual leading-log approximation (LLA), and (ii) realistically add all important kinematic cuts. For (i), we adopted the improved EWA (IEWA)¹³ which includes the exact kinematics for each initial gauge boson. For (ii), we further approximately implemented the cuts for $P_T(VV)$ which is crucial in suppressing the SM backgrounds^{10,14} though it is ignored in all previous EWA-analyses. The full tree-level calculation shows that the $P_T(VV)$ -cut also reduces about one third to half of the fusion-signals. Therefore, only after including the $P_T(VV)$ -cut, the IEWA analysis

^bIn order to get reliable results, the subtleties in handling the kinematic singularities also need special care.

can give a more realistic signal-prediction that is comparable to the full tree-level calculation. The following set of kinematic cuts is imposed in our IEWA-analysis for the WW/ZZ final states at the 1.6(0.8)TeV e^-e^+ and e^-e^- LCs:

$$\begin{aligned}
700(350)\text{GeV} &\leq M_{WW} \leq 1.2(0.6)\text{TeV}, & 700(350)\text{GeV} &\leq M_{ZZ} \leq 1.2(0.6)\text{TeV}, \\
-0.80(-0.80) &\leq \cos\theta(W) \leq 0.80(0.80), & -0.80(-0.80) &\leq \cos\theta(Z) \leq 0.80(0.80), \\
200(100)\text{GeV} &\leq P_T(W) \leq 1.6(0.8)\text{TeV}, & 200(100)\text{GeV} &\leq P_T(Z) \leq 1.6(0.8)\text{TeV}, \\
50(40)\text{GeV} &\leq P_T(WW) \leq 1.6(0.8)\text{TeV}, & 30(30)\text{GeV} &\leq P_T(ZZ) \leq 1.6(0.8)\text{TeV}.
\end{aligned} \tag{8}$$

The other cuts used in the full background-study, like $M_{\text{recoil}} \geq 200(150)\text{GeV}$, hardly affect the signal-rate^{10,14} and thus need not to be included in the IEWA-analysis. The cuts in (8) are proven very effective and they ensure the IEWA analysis in good agreements with the full calculations at the tree-level¹⁴. Furthermore, our IEWA-approach has the advantage of conveniently including the leading loop corrections from the $4V_L$ -amplitudes, typically of the order of $\frac{1}{16\pi^2} \simeq 0.0063 > 0.005$, which is at the *same* order of the NLO parameters (α_n 's). It is shown that a 1.6TeV LC can reach a precision around ± 0.005 or better for α_n 's¹⁴. This makes it essentially necessary to include the leading loop corrections to both the scattering amplitudes and the renormalization running of α_n 's. But, inclusion of the complete loop-level electroweak corrections is unrealistic for the $2 \rightarrow 4$ full calculations so far.

In the following, we focus on the precision test of the $SU(2)_C$ -violating parameters $\alpha_{6,7,10}$ via VV -fusions which were ignored in all previous studies for simplicity [though they are still poorly bounded by the current data (see Sec. 2)]. The appearance of $\alpha_{6,7,10}$ signals the new physics beyond the SM. To probe $\alpha_{6,7}$, we need to measure the cross-section ratio for $W^-W^+ \rightarrow ZZ$ and $W^-W^+ \rightarrow W^-W^+$ since the former contains $\alpha_{6,7}$ while the latter does not. To test α_{10} we must study $ZZ \rightarrow ZZ$ and we can choose $ZZ \rightarrow WW$ as the reference channel since the latter has no α_{10} -dependence. To discriminate the final state ZZ from that of the $WW \rightarrow ZZ$ channel, we shall tag the out-going ee . Define:

$$\begin{aligned}
\widehat{\mathcal{R}}_{67} &\equiv \left[\frac{1}{\sigma_0} \frac{d\sigma}{dM_{ZZ}}(W^-W^+, ZZ) \right] \left[\frac{1}{\sigma_0} \frac{d\sigma}{dM_{WW}}(W^-W^+, W^-W^+) \right]^{-1}, \\
\mathcal{R}_{67} &\equiv \frac{\sigma(W^-W^+, ZZ|\alpha_6, \alpha_7)}{\sigma(W^-W^+, W^-W^+)} , & \mathcal{R}_{10} &\equiv \frac{\sigma(ZZ, ZZ|\alpha_{67} + \alpha_{10})}{\sigma(ZZ, W^-W^+|\alpha_6, \alpha_7)} ,
\end{aligned} \tag{9}$$

where $\alpha_{67} \equiv \alpha_6 + \alpha_7$, the values of $\alpha_{4,5}$ are fixed, and σ_0 in $\widehat{\mathcal{R}}_{67}$ is the leading order cross section for normalization. In Fig. 3(a)-(b), we plot the $\widehat{\mathcal{R}}_{67}$ for the 1.6TeV and 0.8TeV LCs with $\int \mathcal{L} = 200$ & 100fb^{-1} , and the sensitivity to the $SU(2)_C$ -violation effects is shown to differ by about a factor of $O(10)$ on the two machines. In Fig. 3(c)-(d), the ratios \mathcal{R}_{67} and \mathcal{R}_{10} are separately plotted for the 1.6TeV LC (by setting $\alpha_{4,5} = 0$ for simplicity). In plotting the α_{10} - α_6 correlation in Fig. 3(d), we have also fixed α_7 to be zero for simplicity. Here, the realistic cuts in (8) have been imposed and all gauge-boson polarizations are included. Fig. 3 demonstrates that a sensitive probe of $\alpha_{6,7,10}$ down to the level of 10^{-3} can be reached at the 1.6TeV LC with a conservative annual integrated luminosity (200fb^{-1}). The sensitivity is very sensitive to the collider energy and can be enhanced by about an order of magnitude when it is doubled from 800GeV to 1.6TeV. The use of the polarized e^-/e^+ beams will further increase the sensitivity¹⁴.

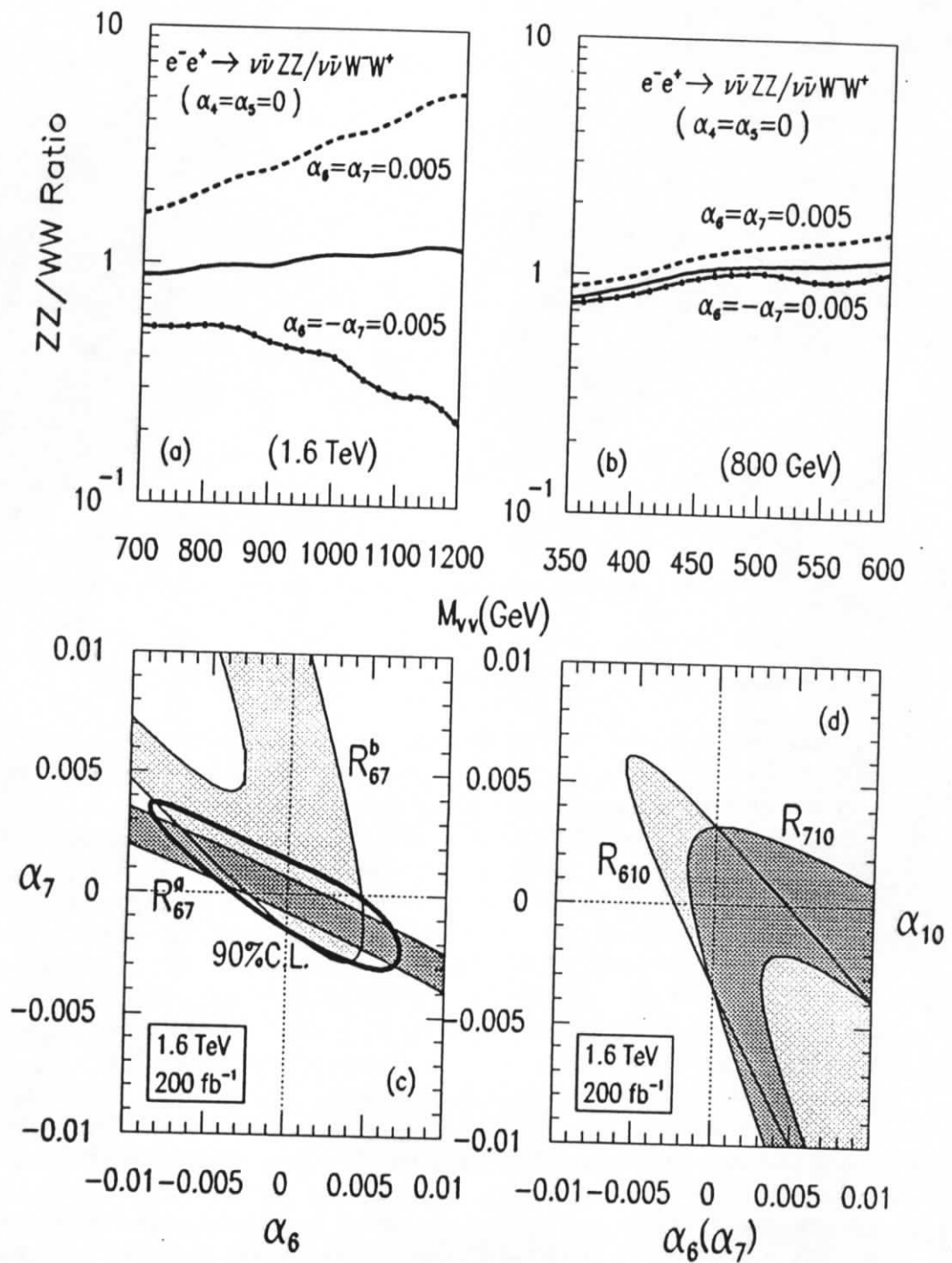


Fig.3. Probing the $SU(2)_c$ violation effects from ZZ/WW ratios.

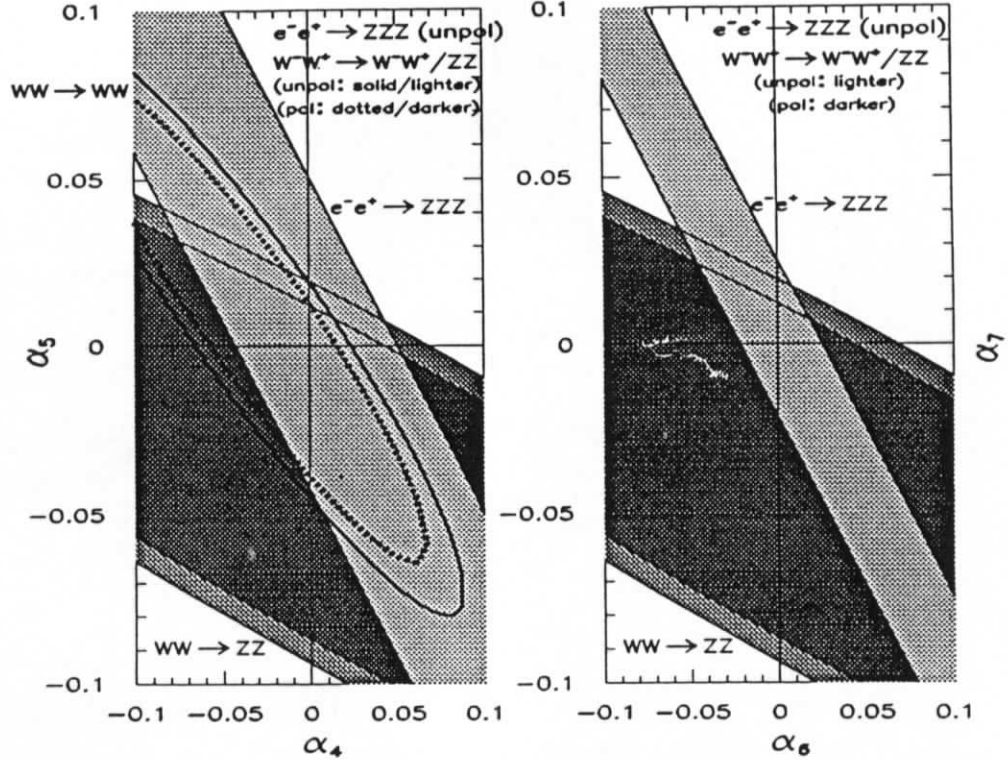


Fig.4. Interplay of the VV and WW productions at 800GeV LC.

5. Interplay of the VV and VVV Productions at the LC

As shown in Table 1, the triple-gauge-boson productions $e^-e^+ \rightarrow ZZZ/W^-W^+Z$ can also probe the QGCs ($\alpha_{4,5,6,7,10}$) via their leading amplitudes. Though the highest E -power dependence of these leading amplitudes is lower than that of the VV -fusions by a factor of 2, the backgrounds for them are greatly reduced: there are only 1(14) background-graphs in the $ZZZ(WWZ)$ production instead of $O(40-50)$ in VV -fusions. So, we expect them becoming important/competitive in relatively lower energy regions. As plotted in Fig. 3(a)-(b), the sensitivity of VV -fusions to the QGCs decreases by about a factor of 10 when the collider energy (1.6TeV) reduced by half (down to 800GeV). The important question to ask is: "At the 800GeV phase of a LC, how do we achieve a meaningful *first-step* direct probe on the QGCs?" A systematic SM calculation for VVV -productions was performed before¹⁶. Here we perform a further analysis for the new physics: the anomalous QGCs ($\alpha_{4,5,6,7,10}$). To save space, we summarize a comparative study for $e^-e^+ \rightarrow ZZZ$ and $W^-W^+ \rightarrow ZZ/WW$ at the LC(0.8TeV) in Fig. 4, where the 1σ -bounds are displayed. It shows that for probing $SU(2)_C$ -conserving parameters $\alpha_{4,5}$ the ZZZ -production is significantly better than $WW \rightarrow ZZ$ fusion (including its polarized case: 100%/50%-polarization for e^-/e^+ -beams) and bounds different ranges of the parameter space, but it is not competitive with $WW \rightarrow WW$ in probing $\alpha_{4,5}$ since it is weaker and bounds in the similar direction. However, for probing $SU(2)_C$ -violating parameters $\alpha_{6,7}$, the situation dramatically changes: the $4W$ -channel (of no $\alpha_{6,7}$ -dependence) is no longer relevant and the ZZZ -production becomes the best and

complementary to the $WW \rightarrow ZZ$ -channel by bounding the different directions of the α_6 - α_7 plane in a much stronger way. Since the sensitivity here is much lower than that of a LC(1.6TeV), we emphasize that it is important to combine both VVV -productions and VV -fusions to achieve a first direct sensitive test on these QGCs. Our systematic analysis is given elsewhere¹⁷.

6. Concluding Remark: the ‘‘Higgs Puzzle’’

All unsuccessful Higgs-searches so far associate our times with a big ‘‘Higgs puzzle’’. Veltman’s screening theorem deepens this ‘‘puzzle’’. Though the direct lower Higgs-mass-bound is gradually pushed up, the unitarity and triviality forbid it to go beyond the TeV scale, at which we are facing an exciting strong EWSB dynamics. Below the new heavy resonance, we must first probe the EWSB parameters formulated by the EWCL. We perform systematic global analysis on how the LHC and LCs complementarily explore the complete set of these parameters by different VV -fusion and $f\bar{f}^{(\prime)}$ -annihilation processes. With this overall physical guideline, we make further precision study on the QGCs with focus on the new $SU(2)_C$ -violation effects. The interplay of VV -fusions and VVV -productions is revealed. Combining different phases and different channels at the LCs and adding together the discovery-power of the LHC, it is possible to achieve a complete test on the strong EWSB dynamics for solving this deep ‘‘Higgs puzzle’’—the 20th century’s gift.

Acknowledgements I thank Bernd Kniehl for invitation and for organizing such a stimulating workshop. I am grateful to Tao Han, C.-P. Yuan and Peter Zerwas for helpful suggestions to my talk, and my further great thanks go to them and other collaborators for the productive collaborations upon which this talk is based. I also thank John Gunion and Kaoru Hagiwara for useful discussions. The work is supported by the AvH of Germany.

1. S. Weinberg, *Physica* **96A** (1979) 327.
2. H. Georgi, *Ann. Rev. Nucl. & Part. Sci.* **43** (1994) 209.
3. J. Bagger, et al, *Phys. Rev.* **D49** (1994) 1246; **D52** (1995) 3878.
4. T. Han, in these proceedings.
5. E.g., C. Hill, *Phys. Lett.* **B345** (1995) 483; R. Casalbuoni, et al, *Phys. Rev.* **D53** (1996) 5201; E.H. Simmons, in these proceedings; and references therein.
6. T. Appelquist, et al, *Phys. Rev.* **D22**, 200 (1980); *Phys. Rev.* **D48**, 3235 (1993).
7. H.-J. He, Y.-P. Kuang, C.-P. Yuan, *Phys. Rev.* **D55** (1997) 3038; *Mod. Phys. Lett.* **A11** (1996) 3061.
8. H.-J. He, Y.-P. Kuang, C.-P. Yuan, *Phys. Lett.* **B382** (1996) 149.
9. H.-J. He, Y.-P. Kuang, C.-P. Yuan, *Phys. Rev.* **D51**, 6463 (1995); H.-J. He and W.B. Kilgore, *Phys. Rev.* **D55** (1997) 1515; H.-J. He, et al, *Phys. Rev. Lett.* **69**, 2619 (1992); *Phys. Rev.* **D49**, 4842 (1994); *Phys. Lett.* **B329**, 278 (1994).
10. V. Barger, K. Cheung, T. Han, R.J.N. Phillips, *Phys. Rev.* **D52** (1995) 3815.
11. K. Hagiwara, private communications; K. Hagiwara, et al, KEK-TH-282, 1991.
12. J.F. Gunion, et al, *The Higgs Hunter’s Guide*, (Addison-Wesley Pub., 1990).
13. P.W. Johnson, F.I. Olness, Wu-Ki Tung, *Phys. Rev.* **D36** (1987) 291.
14. E. Boos, H.-J. He, W. Kilian, C.-P. Yuan, P.M. Zerwas, DESY-96-256.
15. E. Boos, et al, hep-ph/9701412 and hep-ph/9503280.
16. V. Barger, T. Han, R.J.N. Phillips, *Phys. Rev.* **D39** (1989) 146.
17. T. Han, H.-J. He, et al, in preparation.

